Received: 20 June 2024 | Revised: 21 August 2024 | Accepted: 9 September 2024

DOI: 10.1002/kin.21760

RESEARCH ARTICLE

INTERNATIONAL JOURNAL OF CHEMICAL KINETICS WILEY

Decomposition of CH_3NH_2: Implications for CH_x/NH_y radical–radical reactions

Peter Glarborg[1] | **Maria U. Alzueta**[2]

[1]Department of Chemical and Biochemical Engineering, Technical University of Denmark, Lyngby, Denmark

[2]Department of Chemical and Environmental Engineering, Aragon Institute of Engineering Research (I3A), University of Zaragoza, Zaragoza, Spain

Correspondence
Peter Glarborg, Department of Chemical and Biochemical Engineering, Technical University of Denmark, DK-2800 Kgs. Lyngby, Denmark.
Email: pgl@kt.dtu.dk

Funding information
Horizon 2020 Framework Programme, Grant/Award Number: PID2021-12432OBI00

Abstract

Experiments on methylamine (CH_3NH_2) decomposition in shock tubes, flow reactors, and batch reactors have been re-examined to improve the understanding of hydrocarbon/amine interactions and constrain rate constants for CH_x + NH_y reactions. In high-temperature shock tube experiments, the rapid thermal dissociation of CH_3NH_2 provides a fairly clean source of CH_3 and NH_2 radicals, allowing an assessment of reactions of CH_3 with NH_2 and NH. At the lower temperatures in batch and flow reactors, CH_3NH_2 is mostly consumed by reaction with H to form CH_2NH_2 + H_2; these results are useful in determining the fate of the CH_2NH_2 radical. Interpretation of these data, along with flow reactor data for the CH_3NH_2/H system at lower temperature, indicates that at temperatures up to about 1400 K at atmospheric pressure and above 2000 K at 100 atm, the CH_3 + NH_2 reaction forms mainly methylamine. At sufficiently high temperature, H-abstraction to form CH_4 + NH and addition–elimination to form CH_2NH_2 + H become competitive. The CH_3 + NH reaction, with a rate constant close to collision frequency, forms CH_2NH + H, also leading into the hydrocarbon amine pool. Thus, methylamine can be expected to be an important intermediate in co-combustion of natural gas and ammonia, and more work on the chemistry of CH_3NH_2 is desirable.

KEYWORDS
ammonia, CH_3NH_2, decomposition, kinetics

1 | INTRODUCTION

Ammonia is a carbon-free energy carrier that attracts interest as an alternative fuel in engines and gas turbines. In addition to its toxicity and concerns about emissions of nitrogen oxides (both NO_x and N_2O), technical barriers include its poor combustion characteristics.[1–3] Strategies to address this problem involve the use of an additional fuel, for example, hydrogen, natural gas, or diesel, to secure ignition.[4,5]

The co-oxidation of ammonia and methane has been studied intensively in recent years. Ignition delay times have been reported from experiments in rapid compression machines (RCM)[6–9] and shock tubes,[10–12] and results are available also from flow reactors,[13–16] jet-stirred reactors,[15,17–19] and laminar premixed flames (flame speed[20–31] and flame structure[26,32–35]). A comprehensive study of the combustion chemistry of co-combustion of ammonia with C_1-fuels was recently published by Zhang et al.[36]

The chemical coupling between the oxidation of ammonia and methane is still not fully clarified, despite the significant recent research effort. The reactions may either involve H-abstraction,

$$CH_4 + NH_2 \rightleftarrows CH_3 + NH_3 \quad (R30)$$

$$CH_3 + NH_2 \rightleftarrows CH_4 + NH \quad (R31)$$

$$CH_3 + NH_2 \rightleftarrows CH_2 + NH_3$$

$$CH_3 + NH \rightleftarrows CH_4 + N$$

or feed into the hydrocarbon amine pool,

$$CH_3 + NH_2(+M) \rightleftarrows CH_3NH_2(+M) \quad (R1)$$

$$CH_3 + NH_2 \rightleftarrows CH_2NH_2 + H \quad (R11b)$$

$$CH_3 + NH \rightleftarrows CH_2NH + H \quad (R32)$$

The key steps are believed to be the H-abstraction by NH_2 from the hydrocarbon fuel (R30) and the recombination of NH_2 with the primary hydrocarbon radical to form a hydrocarbon amine (R1).

To facilitate an improved quantitative understanding of this reaction subset, experimental results on thermal dissociation of methyl amine (CH_3NH_2) are re-interpreted in terms of the present understanding of the chemistry. The thermal dissociation of CH_3NH_2 has been studied experimentally in batch reactors,[37] flow reactors,[38] and shock tubes.[39–42] With the exception of the flow reactor work, these studies date back 25 years or more. More recent studies on nitrogen chemistry in general[43] and amines in particular[38,44,45] have served to improve our understanding of the elementary steps involved, allowing a more reliable interpretation of the published results. Experiments selected for re-examination in the present work include measurements of NH_2, NH, and H from shock tube experiments,[41,42] stable species concentrations from flow reactor experiments,[38] and pressure measurements from batch reactor experiments.[37] The shock tube studies were designed to determine rate constants for CH_3NH_2 dissociation channels; in the present work, we look at the implications of the experimental results also for rate constants of secondary reactions, mainly the reactions of CH_3 with NH_2 and NH. The batch and flow reactor studies

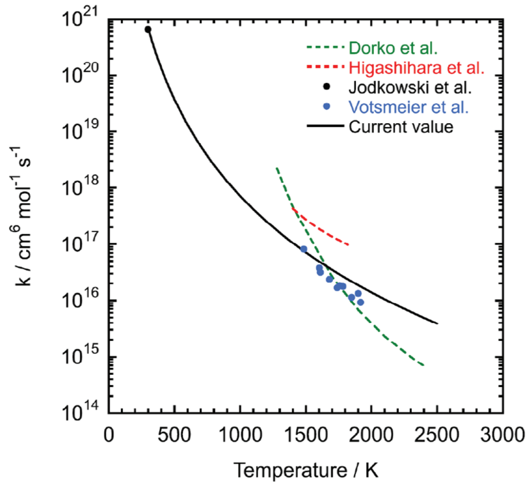

FIGURE 1 Arrhenius plot for the reaction $CH_3 + NH_2 + M \rightleftarrows CH_3NH_2 + M$ (R1). The black symbol denotes a measurement of the low-pressure limit at 300 K by Jodkowski et al.[58] while the dashed lines and the blue symbols denote values of k_1 obtained from high temperature measurements of the reverse step from Dorko et al.,[39] Higashihara et al.,[40] and Votsmeier et al.,[42] converted using the thermodynamic properties. The solid line is the preferred low-pressure limit $k_{1,0}$, based on the data from Jodkowski et al. and Votsmeier et al.

allow us to examine further the initial step (R1), as well as the fate of the CH_2NH_2 radical.

2 | DETAILED CHEMICAL KINETIC MODEL

The core of the chemical kinetic model, including rate coefficients and thermodynamic data, was drawn from the review of nitrogen chemistry by Glarborg et al.,[43] but the H/N/O subset was updated according to Jian et al.[46] while the subset for CH_3NH_2 was drawn initially from Glarborg et al.[45] Table 1 lists selected reactions in the CH_3NH_2 decomposition subset. The full reaction mechanism, as well as thermodynamic data,[43,45] is available as Supplementary Material.

The rate constant for $CH_3 + NH_2$ (+M) $\rightleftarrows$ CH_3NH_2 (+M) (R1) has been measured in the forward direction at room temperature[58] and in the reverse direction (dissociation of CH_3NH_2) at high temperature in shock tube experiments.[39,40,42] The shock tube results were converted from k_{1b} to k_1 using the equilibrium constant. We have based the coefficients for the low-pressure limit on the low-temperature data from Jodkowski et al.[58] and the high temperature data from Votsmeier et al.[42] (Figure 1). The other shock tube data are considered less reliable, because they were obtained under less dilute conditions.

INTERNATIONAL JOURNAL OF CHEMICAL KINETICS

TABLE 1 Selected reactions in the CH_3NH_2 decomposition subset. Parameters for use in the modified Arrhenius expression $k = AT^{\beta} \exp(-E/[RT])$. Units are mol, cm, s, and cal.

		A	*β*	*E*	Source
1.	$CH_3 + NH_2(+M) \rightleftarrows CH_3NH_2(+M)$	1.0E14	0.000	0	See text
	Low pressure limit:	8.2E34	−5.687	0	
	$F_c = 0.5$				
2.	$CH_3NH_2 + M \rightleftarrows CH_4 + NH + M$	2.5E14	0.000	56,500	See text
3.	$CH_3NH_2 + H \rightleftarrows CH_2NH_2 + H_2$	1.6E13	0.000	5300	See text
4.	$CH_3NH_2 + H \rightleftarrows CH_3NH + H_2$	2.0E12	0.000	5300	See text
5.	$CH_3NH_2 + H \rightleftarrows CH_3 + NH_3$	7.8E08	1.170	10,800	45
6.	$CH_3NH_2 + CH_3 \rightleftarrows CH_2NH_2 + CH_4$	1.5E06	1.870	9170	47
7.	$CH_3NH_2 + CH_3 \rightleftarrows CH_3NH + CH_4$	1.6E06	1.870	8842	47
8.	$CH_3NH_2 + NH_2 \rightleftarrows CH_2NH_2 + NH_3$	2.8E06	1.940	5494	47
9.	$CH_3NH_2 + NH_2 \rightleftarrows CH_3NH + NH_3$	1.8E06	1.940	7143	47
10.	$CH_2NH_2 \rightleftarrows CH_2NH + H$	2.2E30	−5.465	44,717	48 (1 atm[a])
11.	$CH_2NH_2 + H \rightleftarrows CH_3 + NH_2$	8.5E13	0.000	0	See text
12.	$CH_2NH_2 + H \rightleftarrows CH_2NH + H_2$	4.8E08	1.500	−894	47
13.	$CH_2NH_2 + CH_2NH_2 \rightarrow$ adduct	8.7E14	−0.700	−3	est[b]
14.	$CH_3NH \rightleftarrows CH_2NH_2$	3.5E37	−7.987	44,942	49 (1 atm[a])
15.	$CH_3NH \rightleftarrows CH_2NH + H$	4.4E25	−4.239	36,163	48 (1 atm[a])
16.	$CH_2NH + H \rightleftarrows H_2CN + H_2$	2.4E08	1.500	7322	47
17.	$CH_2NH + H \rightleftarrows HCNH + H_2$	3.0E08	1.500	6130	47
18.	$CH_3CH_2NH_2 \rightleftarrows C_2H_5 + NH_2$	4.5E12	0.000	63,158	50 (1 atm)
19.	$CH_3CH_2NH_2 \rightleftarrows CH_3 + CH_2NH_2$	2.7E97	−23.520	129,000	51 (1 atm[a])
20.	$CH_3CH_2NH_2 + H \rightleftarrows CH_2CH_2NH_2 + H_2$	1.9E02	3.520	6090	52
21.	$CH_3CH_2NH_2 + H \rightleftarrows CH_3CHNH_2 + H_2$	2.4E13	0.000	5768	52
22.	$CH_3CH_2NH_2 + H \rightleftarrows CH_3CH_2NH + H_2$	2.0E07	1.870	7930	52
23.	$CH_3CH_2NH_2 + CH_3 \rightleftarrows CH_2CH_2NH_2 + CH_4$	4.0E-11	6.860	5135	52
24.	$CH_3CH_2NH_2 + CH_3 \rightleftarrows CH_2CHNH_2 + CH_4$	1.3E-4	4.950	3544	52
25.	$CH_3CH_2NH_2 + CH_3 \rightleftarrows CH_3CH_2NH + CH_4$	4.9E-7	5.760	2594	52
26.	$CH_3CH_2NH_2 + NH_2 \rightleftarrows CH_2CH_2NH_2 + NH_3$	9.2E12	0.000	9386	53
27.	$CH_3CH_2NH_2 + NH_2 \rightleftarrows CH_3CHNH_2 + NH_3$	1.7E12	0.000	4729	53
28.	$CH_3CH_2NH_2 + NH_2 \rightleftarrows CH_3CH_2NH + NH_3$	3.7E11	0.000	5398	53
29.	$C_2H_4 + NH_2 \rightleftarrows CH_2CH_2NH_2$	2.1E10	0.000	2623	54
30.	$CH_4 + NH_2 \rightleftarrows CH_3 + NH_3$	1.5E03	3.010	9940	55
31.	$CH_3 + NH_2 \rightleftarrows CH_4 + NH$	2.3E-4	4.854	1529	56
32.	$CH_3 + NH \rightleftarrows CH_2NH + H$	8.0E13	0.000	0	See text
33.	$^1CH_2 + NH_3 \rightleftarrows {}^3CH_2 + NH_3$	1.0E14	0.000	0	See text

[a]Rate coefficients over a wider pressure range provided in Supplementary Material.
[b]Estimated as $C_2H_5 + C_2H_5$.[57]

Under the conditions of the shock tube experiments of Votsmeier et al., reaction R1 is possibly slightly into the fall-off region. We have interpreted their data assuming a high pressure limit of $k_{1,\infty} = 1.0 \cdot 10^{14}$ cm^3 mol^{-1} s^{-1}, independent of temperature. This value is compatible with the determination of Jodkowski et al. at 300 K, but significantly below that calculated recently by de Jesus et al.[59] The low pressure limit $k_{1,0}$ was then adjusted to obtain agreement with the reported values from Votsmeier et al. for the resulting value of k_1. Further work is desirable to characterize more accurately the temperature and pressure dependence of R1, as well as the collision efficiency of various molecules.

Based on NH-measurements in shock tube decomposition of CH_3NH_2, Klatt et al.[41] proposed a minor dissociation channel forming CH_4 + NH (R2). An NH-forming channel could be a direct reaction or perhaps result from initial formation of $CH_3 + NH_2$, followed by a roaming step to form the final products. We have tentatively included the reaction with a rate constant at 1850 K to match the measured early NH-profile reported by Klatt et al. (see Figure 9 below), applying an activation energy similar to that of the main dissociation channel R1b.[42] Klatt et al. show from measurements of the H-atom profiles that dissociation of CH_3NH_2 to $CH_2NH_2 + H$ is insignificant.

Reactions of CH_3NH_2 with the radical pool under pyrolysis conditions include

$$CH_3NH_2 + H \rightarrow \text{products} \qquad (R3,R4,R5)$$

$$CH_3NH_2 + CH_3 \rightarrow \text{products} \qquad (R6,R7)$$

$$CH_3NH_2 + NH_2 \rightarrow \text{products} \qquad (R8,R9)$$

These steps mostly involve H-abstraction, with attack on the CH_3-site being favored due to a lower barrier. Accordingly, CH_2NH_2 is formed in larger amounts than CH_3NH. The overall rate constant k_{tot} for CH_3NH_2 + H was measured at 473–683 K by Blumenberg and Wagner.[60] In addition, several ab initio studies have been reported.[61–63] Figure 2 shows an Arrhenius plot for the reaction. The calculated values by Kerkeni and Clary[62] are in reasonable agreement with the experimental study of Blumenberg and Wagner, while the other theoretical studies[61,63] imply rate constants that are faster than the experimental values, but possibly within their uncertainty. The present modeling study supports a direct extrapolation to higher temperature of the overall rate constant of Blumenberg and Wagner (see below). We have adopted their value for k_{tot}, combining it with the branching fraction $k_3/(k_3 + k_4)$ of 90% as calculated by Kerkeni and Clary. Glarborg et al.[45] investigated theoretically the possible importance of a channel to $CH_3 + NH_3$ (R5), but found it to be too slow to compete with H-abstraction.

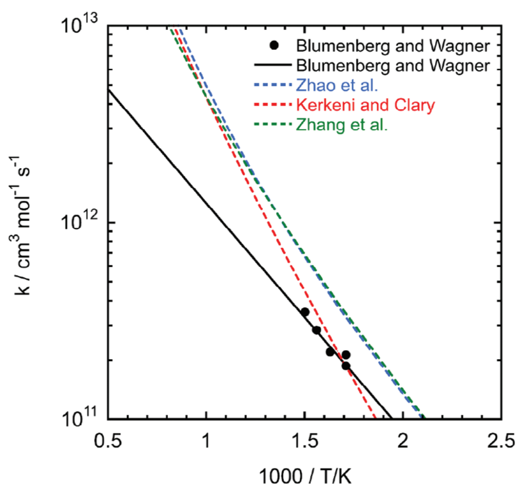

FIGURE 2 Arrhenius plot for the reaction $CH_3NH_2 + H \rightarrow$ products. The symbols and solid line show the experimental results for the overall reaction from Blumenberg and Wagner[60] while the dashed lines denote theoretical values from Zhao et al.[61], Kerkeni and Clary,[62] and Zhang et al.[63]

For the reactions of CH_3NH_2 with CH_3 (R6, R7) and NH_2 (R8, R9), we have adopted the QRRK estimates of Dean and Bozzelli.[47] For $CH_3NH_2 + CH_3$, the sum of the rate constants is in good agreement with the overall rate reported by Gray and Thynne[64,65] at 383–453 K, but the extrapolation to high temperature is uncertain. For $CH_3NH_2 + NH_2$, there are no experimental data reported. A recent theoretical study by Rawadief et al.[53] indicates rate constants that are significantly lower than those proposed by Dean and Bozzelli.

In the absence of O_2, the radicals CH_2NH_2 and CH_3NH would be expected mainly to dissociate thermally at combustion temperatures. The rate constants for thermal dissociation

$$CH_2NH_2 \rightleftarrows CH_2NH + H \qquad (R10)$$

$$CH_3NH \rightleftarrows CH_2NH + H \qquad (R15)$$

were recently calculated by Sun et al.[48] over a wide range of temperature and pressure and we have adopted their values. Isomerization (R14) is too slow to compete with the H-elimination steps.[48,49]

Due to its low thermal stability, the reactions of CH_2NH_2 with the radical pool are of interest mainly if the reverse reaction plays a role in the hydrocarbon/amine chemical coupling. For example, the reaction of CH_2NH_2 with H yields $CH_3 + NH_2$,

$$CH_2NH_2 + H \rightleftarrows CH_3 + NH_2 \qquad (R11)$$

Reaction R11 competes with direct H-abstraction,

$$CH_2NH_2 + H \rightleftarrows CH_2NH + H_2 \qquad (R12)$$

The branching fraction between these two channels, defined as $\alpha = k_{11}/(k_{11} + k_{12})$, can be estimated from the results of Blumenberg and Wagner.[60] They determined the relative yield of N_2 in the CH_3NH_2/H reaction system when adding different levels of NO (Figure 3). Since NH_2 reacts rapidly with NO,[43]

$$NH_2 + NO \rightleftarrows N_2 + H_2O$$

$$NH_2 + NO \rightleftarrows N_2 + H + OH$$

the N_2 yield is a measure of the NH_2 formed. At the low temperatures of their experiments (473–683 K), reaction R11 is the only important source of NH_2, since thermal dissociation of CH_3NH_2 (R1) is insignificant.

INTERNATIONAL JOURNAL OF CHEMICAL KINETICS

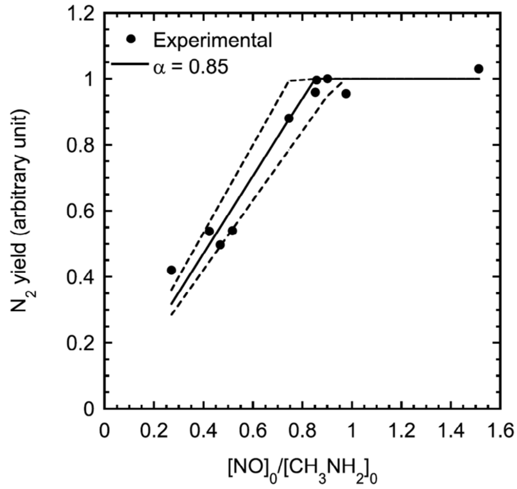

FIGURE 3 The relative yield of N_2 in the CH_3NH_2/H reaction system when adding different levels of NO. The symbols denote the measured by Blumenberg and Wagner,[60] while the solid line denotes the correlation $f(N_2) = ([NO]_0/[CH_3NH_2]_0)/\alpha$ (for $f(N_2) \leq 1$), where $f(N_2)$ is the relative fraction of N_2 and α is the branching fraction for the CH_2NH_2 + H reaction, defined as $k_{11}/(k_{11} + k_{12})$. The dashed lines show the effect of varying α as 0.85 ± 0.1.

The N_2 yield, thus, provides a measure of the branching fraction for the CH_2NH_2 + H reaction, since $\alpha \simeq [NO]_0/[CH_3NH_2]_0$ when the N_2 yield reaches its maximum. From the data in Figure 3, we estimate a value of α of about 85%. The overall rate constant for CH_2NH_2 + H is not known, but it can be assumed to be very fast. Adopting a QRRK estimate for k_{12},[47] we arrive at a value of k_{11} close to collision frequency (Table 1). The estimated uncertainty in k_{11} is a factor of 2.5.

Other product channels for CH_2NH_2 + H can be disregarded. Based on the results of Klatt et al.[41] discussed above, recombination of CH_2NH_2 and H to form CH_3NH_2 is insignificant; the rate constant must be considerably lower than that of the similar reaction C_2H_5 + H (+M). Formation of methylene and ammonia is not likely to be a major channel either. The reaction $^1CH_2 + NH_3 \rightarrow$ products would be expected to be fast, similar to other reactions of singlet methylene with stable species.[43] If it proceeded by addition–elimination to form CH_2NH_2 + H, being almost thermo-neutral, it would be very fast also in the reverse direction. However, there are no indications of CH_2NH_2 + H forming singlet methylene to any significant extent.[60] Consequently, we assume that $^1CH_2 + NH_3$ mostly proceeds through intersystem crossing (ISC) to form $^3CH_2 + NH_3$ (R33), similar to reactions of $^1CH_2$ with O_2, H_2O, and N_2.[43]

Other reactions of CH_2NH_2 of interest include the self-reaction,

$$CH_2NH_2 + CH_2NH_2 \rightarrow \text{adduct} \quad \text{(R13)}$$

This step may become important under undiluted conditions at not too high temperature, such as decomposition of pure CH_3NH_2 in a batch reactor.[37] In the absence of any experimental or theoretical data on the reaction, its rate constant was assumed to be similar to that of C_2H_5 recombination, which is at its high pressure limit even at fairly low pressure.[57]

A major motivation for the present study was to re-interpret global experiments on CH_3NH_2 decomposition to constrain rate constants for radical-radical reactions coupling the hydrocarbon/amine chemistry; mainly the reactions of CH_3 with NH_2 and NH. In addition to recombination (R1) and formation of CH_2NH_2 + H (R11b), CH_3 + NH_2 may proceed as an H-abstraction reaction,

$$CH_3 + NH_2 \rightleftarrows CH_4 + NH \quad \text{(R31)}$$

This step has been measured in the reverse direction at high temperature by Rohrig and Wagner,[66] while no data have been reported in the forward direction. Theoretical values by Dean and Bozzelli[47] from QRRK estimation and by Xu et al.[56] from ab initio calculations (chosen in the present work) are both in good agreement with experiment (Figure 4).

The CH_3 + NH reaction is expected to be very fast, but only an estimate of the rate constant is available.[47] Presumably, it proceeds through addition–elimination rather than H-abstraction,

$$CH_3 + NH \rightleftarrows CH_2NH + H \quad \text{(R32)}$$

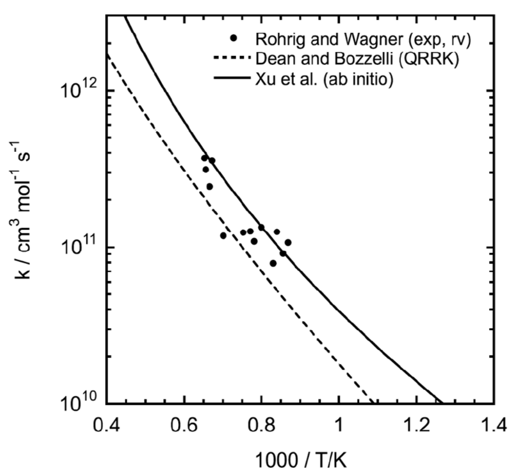

FIGURE 4 Arrhenius plot for the reaction $CH_3 + NH_2 \rightleftarrows CH_4$ + NH (R20). The black symbols denote measurements by Rohrig and Wagner[66] of the reverse step, converted using the thermodynamic properties. The lines show the theoretical values obtained from QRRK[47] and ab initio[56] calculations, with the latter value preferred in the present work.

We have adopted a value of k_{32} based on the measured NH-profile in the CH_3NH_2 decomposition shock tube experiment reported by Klatt et al.[41] (see discussion below). Reactions of radicals with stable species (CH_4 or NH_3) are less important in pyrolysis of CH_3NH_2, but are included in the mechanism for completeness; these include $CH_4 + NH_2 \rightleftarrows CH_3 + NH_3$ (R30).[55]

Reactions in the $CH_3CH_2NH_2$ subset may also have implications for decomposition of CH_3NH_2. Higher amines may be formed by recombination of CH_3 and CH_2NH_2 or by reaction of C_2-hydrocarbons with the amine pool. The core of this subset was drawn from the work of Lucassen et al.,[44] but selected reactions were revised in the present work. The thermal dissociation of $CH_3CH_2NH_2$ has been studied both experimentally and theoretically. Figure 5 compares the NH_2 measurements in a shock tube from Li et al.[50] with the calculated values from Almatarneh et al.[67] and Zhang et al.[51] The reaction has two product channels: $C_2H_5 + NH_2$ (R18) and $CH_3 + CH_2NH_2$ (R19). There are major discrepancies between the experimental results and the theoretical work. For R18, we rely tentatively on the measured value from Li et al. (atmospheric pressure); the calculated rate constant from Zhang et al. is almost an order of magnitude faster and appear to be incompatible with the shock tube study. For the second channel, there is better agreement and we adopt the rate coefficients from Zhang et al. since they cover a wide range of pressure and temperature.

Reactions of $CH_3CH_2NH_2$ with the radical pool (H, NH_2, CH_3) have only been studied theoretically[52,53,68] and there are significant differences between the reported rate constants. We have tentatively adopted values from Pappijn et al.[52] and Rawadieh et al.[53]

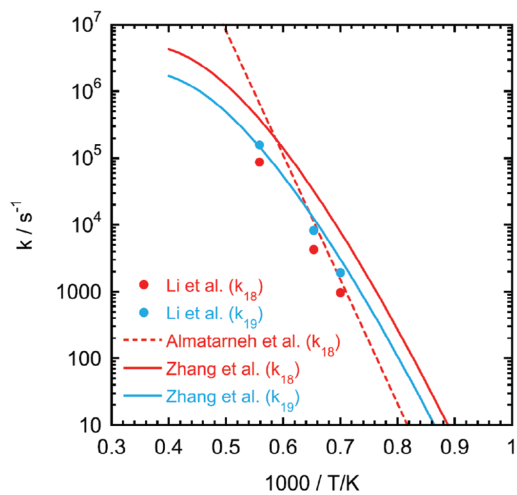

FIGURE 5 Arrhenius plot for the reaction $CH_3CH_2NH_2 \rightarrow C_2H_5 + NH_2$ (R18) or $CH_3 + CH_2NH_2$ (R19) at 1 atm. The symbols denote measurements by Li et al.[50] while the lines show the theoretical values obtained by Almatarneh et al.[67] and Zhang et al.[51]

3 | RESULTS AND DISCUSSION

3.1 | Shock tube experiments

The most reliable shock tube results on methylamine decomposition are those reported by Votsmeier et al.[42] and Klatt and Wagner.[41] These studies, conducted in the temperature range 1780–1850 K and pressures of 0.5–1.6 atm, involved measurements of concentration profiles for the radicals NH_2, NH, and H. Under these conditions, CH_3NH_2 largely dissociates to form $CH_3 + NH_2$ (R1), while H-abstraction reactions with the radical pool leading to CH_2NH_2 or CH_3NH are insignificant. Figure 6 shows a pathway diagram for CH_3NH_2 conversion. Due the high yield of CH_3 and NH_2, the shock tube data are useful for investigating CH_x/NH_y radical–radical reactions, that is, $CH_3 + NH_2$, $CH_3 + NH$, and $NH_2 + NH_2$.

Figure 7 compares the measurements of NH_2 by Votsmeier et al.[42] with modeling predictions. The data were obtained with 100 ppm CH_3NH_2 in Ar at 1.63 atm and 1782 K. As discussed above, our preferred rate constant for R1 is largely based on their work, but their results are also of value in evaluating the ability of the model to describe CH_x/NH_y radical reactions.

The model predicts well the initial formation and the peak concentration of NH_2, while its consumption rate at longer reaction times is slightly underestimated. The NH_2 concentration is a result of the competition between

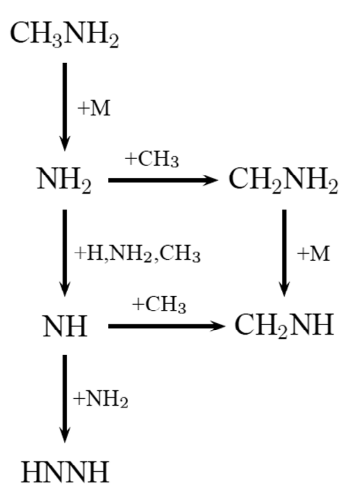

FIGURE 6 Pathway diagram for decomposition of CH_3NH_2 under very dilute conditions in a shock tube in the temperature range 1780–1850 K and pressures of 0.5–1.6 atm.

INTERNATIONAL JOURNAL OF CHEMICAL KINETICS

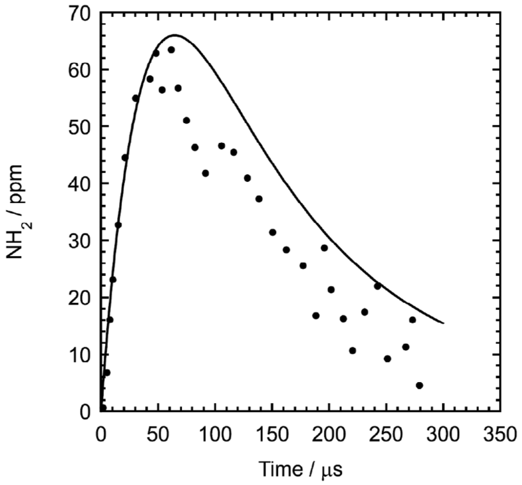

FIGURE 7 Comparison of the shock tube measurements of NH_2 by Votsmeier et al.[42] with modeling predictions in decomposition of CH_3NH_2. Experimental conditions: 100 ppm CH_3NH_2 in Ar at 1.63 atm and 1782 K.

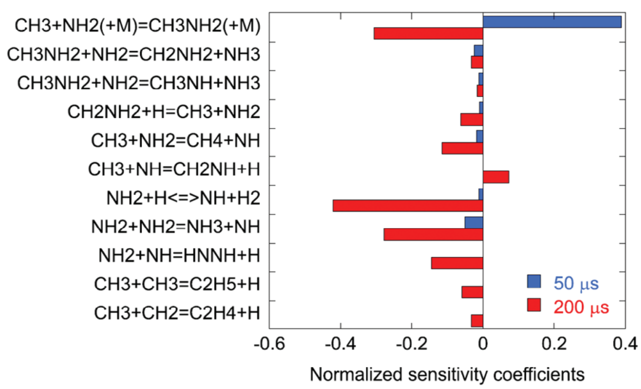

FIGURE 8 Sensitivity analysis for NH_2 for the conditions of Figure 7 (100 ppm CH_3NH_2 in Ar at 1.63 atm and 1782 K).

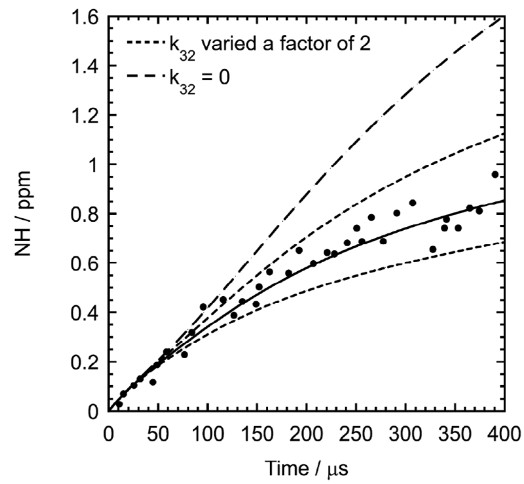

FIGURE 9 Comparison of the shock tube measurements of NH by Klatt et al.[41] with modeling predictions in decomposition of CH_3NH_2. Experimental conditions: 28.1 ppm CH_3NH_2 in Ar at 0.52 atm and 1851 K. The solid line shows predictions with the preferred rate constant for CH_3 + NH of $k_{32} = 8.0 \cdot 10^{13}$ cm^3 mol^{-1} s^{-1}, while the short-dashed lines and the long-dashed line show the effect of varying it by a factor or two and setting it equal to 0, respectively.

formation by thermal dissociation of CH_3NH_2 (R1) and consumption reactions (Figure 6). Figure 8 shows the results of a sensitivity analysis for NH_2 at 50 and 200 μs, respectively, for the conditions of Figure 7. At short reaction times, the NH_2 profile is mainly sensitive to R1, and the good agreement between experiment and predictions supports the current value of k_1. At longer reaction times, NH_2 becomes more sensitive to its consumption reactions. These are mostly radical–radical steps, with the most important being $NH_2 + H \rightleftarrows NH + H_2$ and $NH_2 + NH_2 \rightleftarrows NH_3 + NH$. However, also reactions of NH_2 with CH_3 (R11b, R31), CH_3NH_2 (R8), and NH show up with smaller coefficients. Because R1 promotes formation of chain carriers, the sign of its sensitivity coefficient changes from positive at short reaction times (where NH_2 formation through R1 dominates) to negative at longer times (where consumption of NH_2 by reaction with other radicals is predominant).

The reason for the slight underprediction of the NH_2 consumption rate at longer times is not clear. The rate constants for the reactions of NH_2 with H and with itself are fairly well established, with consistent measurements in both the forward and reverse directions,[69] while that for NH_2 + NH is still in discussion. Apart from k_1, the sensitivity towards $CH_3 + NH_2$ is insufficient to constrain its rate coefficients.

Figure 9 compares modeling predictions with the measurements of NH by Klatt and Wagner.[41] Their focus was mainly on investigating minor secondary dissociation channels for CH_3NH_2, that is, an NH-forming channel and direct H-elimination. Their results, with no delay in formation of NH, support that dissociation of CH_3NH_2 does indeed include a minor direct formation channel to CH_4 and NH (R2). At longer times, other reactions become the dominant sources of NH; these include $CH_3 + NH_2 \rightleftarrows CH_4 + NH$ (R31), $NH_2 + H \rightleftarrows NH + H_2$, and $NH_2 + NH_2 \rightleftarrows NH_3 + NH$.

Figure 10 shows a sensitivity analysis for NH for the conditions of Figure 9. At short reaction times, the predicted NH concentration is only sensitive to the formation from R2. At longer times, the other steps forming NH become dominant; that is, $CH_3 + NH_2$ (R31), NH_2 + H, and $NH_2 + NH_2$. Also the major steps consuming NH show up as sensitive, primarily CH_3 + NH (R32) and NH_2 + NH.

The sensitivity towards the CH_3 + NH reaction is of particular interest, since its rate constant has not previously

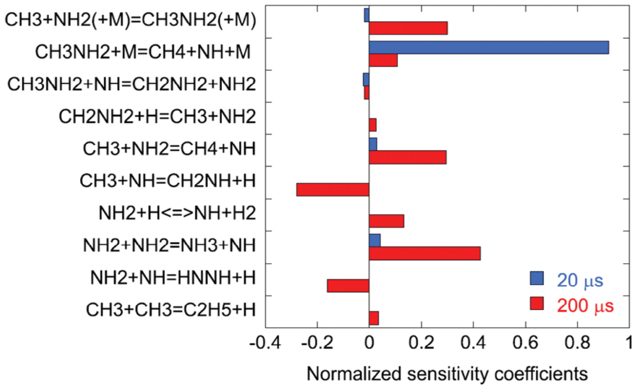

FIGURE 10 Sensitivity analysis for NH for the conditions of Figure 9 (28.1 ppm CH_3NH_2 in Ar at 0.52 atm and 1851 K).

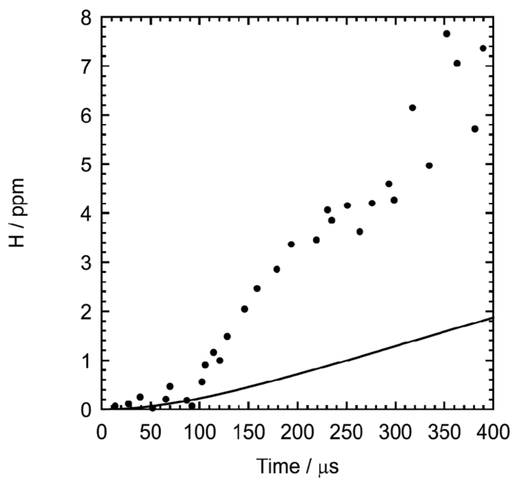

FIGURE 11 Comparison of the shock tube measurements of H by Klatt and Wagner[41] with modeling predictions in decomposition of CH_3NH_2. Experimental conditions: 19.2 ppm CH_3NH_2 in Ar at 0.54 atm and 1840 K.

been determined. The NH-profile from Klatt and Wagner indicates that R32 is very fast; the best agreement is obtained with $k_{32} = 8.0 \cdot 10^{13}$ cm^3 mol^{-1} s^{-1}. The dashed lines on Figure 9 illustrate the impact of varying the value of k_{32} in the modeling predictions.

Figure 11 presents results for atomic H from Klatt and Wagner. The measurements indicate a delay of about 100 μ s in the rapid formation of H, showing that direct H-elimination from CH_3NH_2 is insignificant. At reaction times above 100 μ s, a strong increase in the H-concentration was detected.

The modeling predictions strongly underpredict H at longer reaction times; roughly by a factor of four. Since CH_3NH_2 dissociates rapidly to CH_3 and NH_2 (Figure 6), the H-formation must result mainly from reactions involving these radicals. These include $CH_3 + CH_3 \rightarrow C_2H_5 + H$, $CH_3 + NH_2 \rightarrow CH_2NH_2 + H$ (R11b), and $NH_2 + NH_2 \rightarrow N_2H_3 + H$. To bring the predictions in agreement with the observed H-yield, one of these steps would have to be an order of magnitude faster (see the sensitivity analysis in Figure 12). An error in one of the rate constants of this magnitude is unlikely. The rate constant for the dissociative recombination of CH_3 is known quite accurately at the temperature of Figure 9 (1840 K) from shock tube experiments.[70,71] The reaction $NH_2 + NH_2 \rightarrow N_2H_3 + H$ has been shown by theory to occur without barrier in the reverse direction.[72] Common for these steps is that they are all endothermic, with reverse rate constants of around 10^{14} cm^3 mol^{-1} s^{-1}, that is, close to collision frequency. The only way their rate could be significantly faster and thus improve the agreement of modeling predictions with experiment was if there was a significant error in the thermodynamic properties of one the involved species. This is unlikely, however. Even the heat of formation of CH_2NH_2 is known quite accurately ($\pm$ 0.1 kcal mol^{-1}).[73,74]

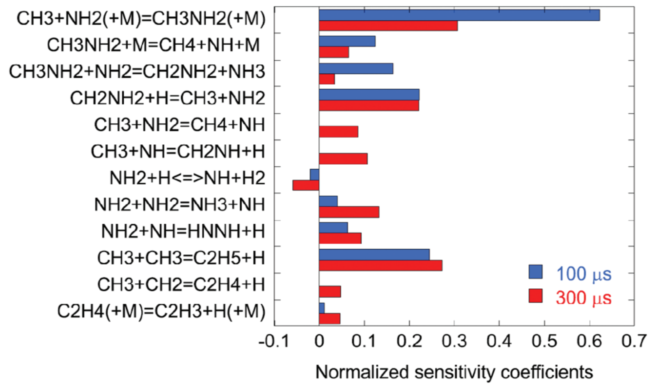

FIGURE 12 Sensitivity analysis for H for the conditions of Figure 11 (19.2 ppm CH_3NH_2 in Ar at 0.54 atm and 1840 K).

Other reactions showing up in the sensitivity analysis include the dissociation steps for CH_3NH_2 (R1, R2), with the largest impact at short times, and the fast reactions of NH with CH_3 (R32) and NH_2. At this point, it is difficult to explain the large discrepancy between calculations and measurements.

The shock tube measurements of CH_3NH_2 decomposition reported by Dorko et al.[39] and Higashihara et al.[40] were obtained at higher CH_3NH_2 concentrations (1%–5%), using IR detection to quantify selected species profiles. Cross-interference between species with C–H bonds complicates the analysis of these data sets. Figure 13 compares results for CH_3NH_2 and NH_3 by Dorko et al.,[39] as extracted by Higashihara et al.,[40] with modeling predictions. Since the experiments were less dilute (1% CH_3NH_2) and conducted at lower temperature (1635–1678 K) and higher pressure (about 4.5 atm), they involved a more complex secondary chemistry, with formation of CH_2NH_2 being significant.

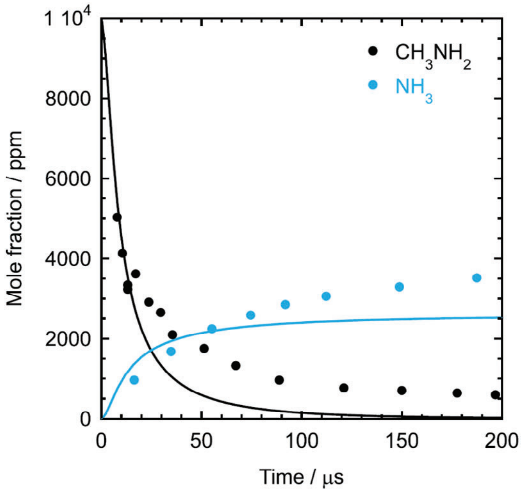

FIGURE 13 Comparison of the shock tube measurements of CH_3NH_2 and NH_3 by Dorko et al.[39] with modeling predictions in decomposition of CH_3NH_2. Experimental conditions: 1% ppm CH_3NH_2 in Ar at 4.57 atm and 1678 K (CH_3NH_2) and 4.41 atm and 1635 K (NH_3), respectively. The experimental data were extracted from the original work by Higashihara et al.[40]

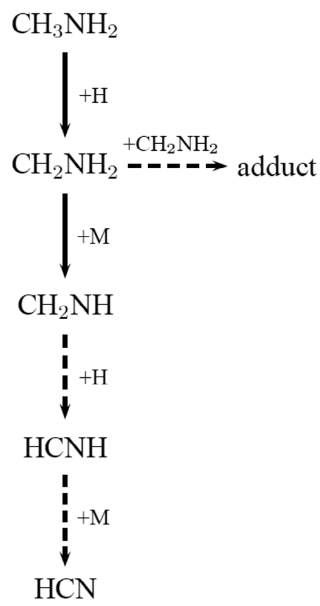

FIGURE 14 Pathway diagram for decomposition of CH_3NH_2 in a batch or flow reactor in the temperature range 900–1200 K at varying pressure and degree of dilution.

The agreement between measurements and modeling predictions is satisfactory, considering the complexity of the chemistry and the experimental uncertainty. The initial slope of CH_3NH_2 is captured by the model, supporting the present value of k_1. The fact that the observed CH_3NH_2 does not approach zero indicates cross-interference with intermediates and products formed, affecting the profile at longer times. At the temperature of these experiments, dissociation of CH_3NH_2 is slower and secondary reactions with radicals play a role. Most of the predicted NH_3 is formed by the H-abstraction reaction between CH_3NH_2 and NH_2. The reasonable agreement for NH_3 between measurement and predictions supports the QRRK estimate for $CH_3NH_2 + NH_2$, as opposed to the significantly lower value calculated by Rawadief et al.[53]

3.2 | Flow reactor and batch reactor experiments

Experimental results on CH_3NH_2 decomposition in reactors are quite limited. The thermal dissociation of CH_3NH_2 has been studied by Emeleus and Jolley[37] in a batch reactor and very recently by Marrodán et al.[38] in a flow reactor. Both studies were conducted at temperatures of 900–1200 K. In this range, the decomposition chemistry of CH_3NH_2 is quite different from that of the shock tube experiments, as shown in the reaction pathway diagram in Figure 14.

The lower temperatures result in a slower thermal dissociation of CH_3NH_2, and consequently CH_3 and NH_2 are formed only in small concentrations. Instead, the decomposition proceeds mainly through a sequential H-abstraction/H-elimination sequence, forming HCN as the final product if the reaction proceeds to completion. The reactor experiments allow us to examine further the initial step (R1), as well as the fate of CH_2NH_2.

Marrodán et al.[38] investigated CH_3NH_2 pyrolysis in a flow reactor at atmospheric pressure. They quantified the reactant CH_3NH_2 and the main products HCN and H_2, along with minor species such as CH_4, NH_3, and CH_2NH. Figure 15 compares their measurements of the major species with modeling predictions.

Marrodán et al. reported that it was challenging to capture the experimental results by the kinetic model, which, similar to the present mechanism, was based on the work of Glarborg et al.[45] Both in their work and in the current study, the initial modeling predictions involved a much faster conversion of CH_3NH_2 than observed experimentally. The discrepancy could conceivably be attributed to erroneous rate constants for CH_3NH_2 dissociation (R1), its reaction with H (R2-R4), or to subsequent reactions of CH_2NH_2; mainly its thermal dissociation (R10) (see the sensitivity analysis in Figure 16). Marrodán et al. concluded that the most uncertain rate constant among these was the QRRK estimate[47] used by Glarborg et al. for $CH_2NH_2 + M \rightleftarrows CH_2NH + H + M$ (R10), and they reduced this value to improve agreement with experiment.

In the present work, we adopted the rate constant for R10 calculated recently by Sun et al.[48] Being more

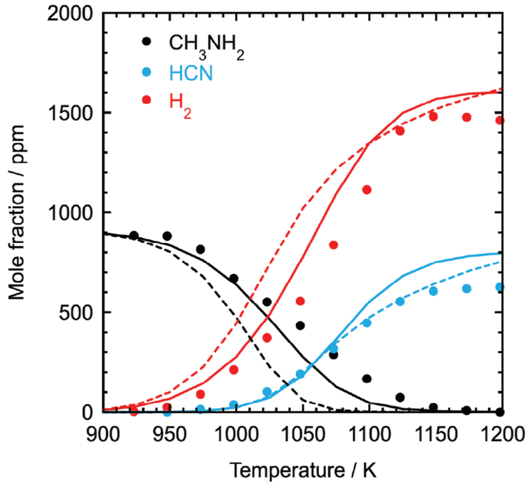

FIGURE 15 Comparison of experimental and predicted mole fractions for decomposition of CH_3NH_2 in a flow reactor. The experimental data are taken from Marrodán et al.[38] The symbols mark experimental data while the lines denote modeling predictions with the model with the rate coefficients for CH_3NH_2 + H (R3, R4) from Blumenberg and Wagner[60] (solid line, preferred) and Kerkeni and Clary[62] (dashed line), respectively. Experimental conditions: inlet composition is 905 ppm CH_3NH_2, 2650 ppm H_2O; balance Ar; pressure 1.0 atm, residence time $\tau(s) = 195$ / T(K) (constant mass flow).

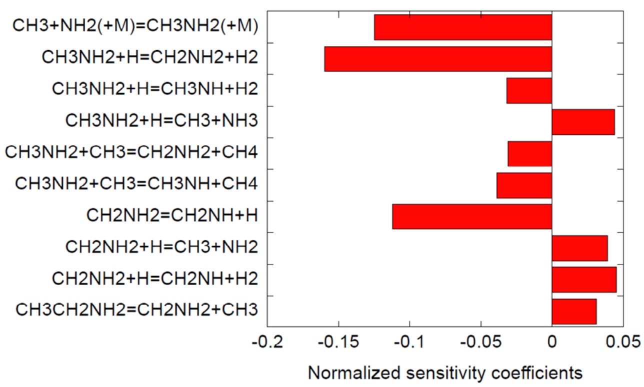

FIGURE 16 Sensitivity analysis for CH_3NH_2 for the conditions of Figure 15 (905 ppm CH_3NH_2, 2650 ppm H_2O in Ar at 1.0 atm, 1000 K).

reliable than the QRRK estimate, this value still has some uncertainty due to the lack of experimental calibration. However, in line with the QRRK estimate, the work of Sun et al. indicates that the reaction is so fast that it under most conditions, particularly in the absence of O_2, would dominate consumption of CH_2NH_2.

To improve the modeling predictions, we tentatively adopt the measured rate coefficients for CH_3NH_2 + H (R3, R4) from Blumenberg and Wagner,[60] instead of the theoretical values from Kerkeni and Clary[62] preferred in our previous work.[38,45] While the two sets of rate constants agree reasonably well at the temperatures of the experiments of Blumenberg and Wagner (473–683 K), they deviate strongly at higher temperatures (Figure 2). The dashed lines in Figure 15 show the effect of replacing the preferred values with those of Kerkeni and Clary. However, due to the sensitivity to other reactions (Figure 16), the results are not conclusive with respect to k_3 and k_4, and it would be desirable to extend the experimental characterization of the CH_3NH_2 + H reaction to higher temperature.

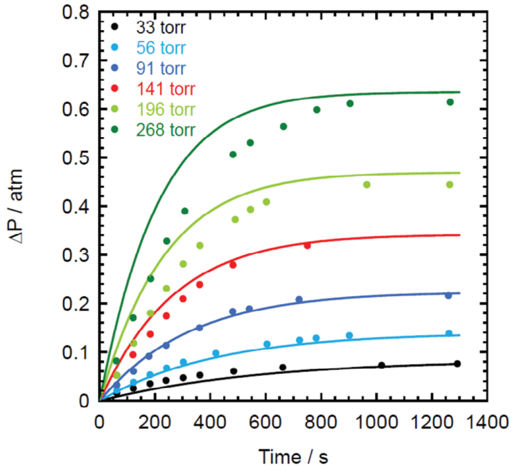

FIGURE 17 Comparison of experimental and predicted pressure increase in decomposition of CH_3NH_2 in a quartz batch reactor. The experimental data are taken from Emeleus and Jolley.[37] The symbols mark experimental data while solid lines denote model predictions. Conditions: starting pressure P_0 varying; inlet composition pure CH_3NH_2.

The reaction progresses according to the pathway diagram in Figure 14. Initially, methylamine is converted through the sequence $CH_3NH_2 \xrightarrow{+H} CH_2NH_2 \xrightarrow{+M} CH_2NH$. At lower temperatures, the concentration of CH_2NH builds up, but above 1050 K, it is converted to HCN through the sequence $CH_2NH \xrightarrow{+H} HCNH \xrightarrow{+M} HCN$ (shown as dashed lines in Figure 14).

With the modified rate constant for CH_3NH_2 + H (R3, R4), the predictions agree well with the measured concentration profiles for the major species. Marrodán et al. did not detect CH_4 (<10 ppm). The data for NH_3 and CH_2NH were associated with a higher uncertainty due to possible cross-interference. Accordingly, we do not show comparisons between modeling predictions and measurements for these minor species.

Emeleus and Jolley[37] conducted batch reactor experiments with pure CH_3NH_2, varying the starting pressure P_0 in the range 33–268 torr. The progress of reaction was monitored by detecting the pressure increase ΔP. Figure 17 compares their results at 890 K with modeling predictions. The agreement is satisfactory, considering the experimental and kinetic uncertainties for these conditions. Emeleus

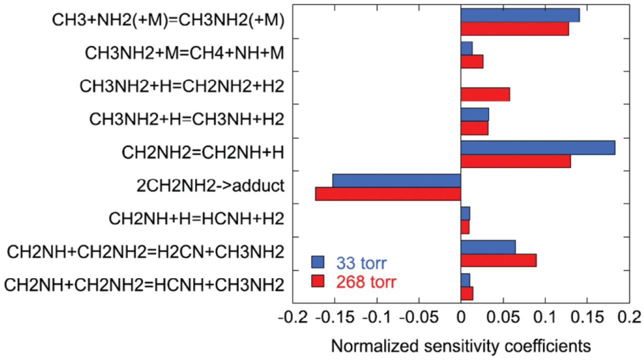

FIGURE 18 Sensitivity analysis for the predicted pressure P for the conditions of Figure 17 (pure CH_3NH_2, 890 K, 200 s).

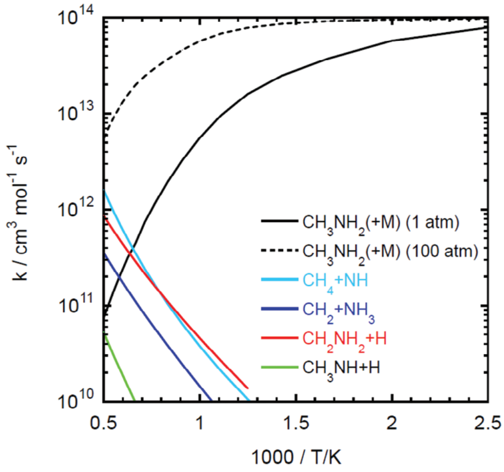

FIGURE 19 Arrhenius plot for the reaction $CH_3 + NH_2 \rightarrow$ products at pressures of 1 and 100 atm. The channel to $CH_2NH + H_2$ has a high barrier[47] and is not shown.

and Jolley investigated the impact of surface activity by conducting experiments in empty and packed reactors. They found that an increased surface/volume ratio affected the competition between dehydrogenation ($CH_3NH_2 \rightarrow HCN + 2H_2$) and hydrogenation ($CH_3NH_2 + H_2 \rightarrow CH_4 + NH_3$). In a packed bed, formation of CH_4 was strongly promoted, reducing the pressure increase. However, in the empty reactor used for the experiments in Figure 17, we expect the surface interaction to be limited.

In addition to experimental concerns, there are considerable uncertainties in the modeling. The dissociation of CH_3NH_2 (R1b) is in the fall-off region under these conditions, and its fall-off behavior is uncertain. Furthermore, by analogy with CH_4 and NH_3,[75,76] CH_3NH_2 would be expected to have a significantly larger collision efficiency than Ar. With initially pure methylamine, this would have a major impact on the rate of thermal dissociation of CH_3NH_2 (R1b) and CH_2NH_2 (R10). We have tentatively assumed a collision efficiency of CH_3NH_2 compared to Ar of 5, with an uncertainty of about a factor of 2.

Another issue is the fate of the CH_2NH_2 radical. At 890 K, the thermal dissociation (R10) is sufficiently slow that other consumption reactions may be competitive. In the course of analyzing the data from Emeleus and Jolley, we found that a strongly terminating step was required to explain the pressure dependence. We believe that recombination of CH_2NH_2 to form an adduct (R13) may play an important role and included this step with a rate constant similar to that of C_2H_5 recombination.

Figure 18 shows the sensitivity of the predicted pressure towards the key steps in the reaction mechanism for the conditions of Figure 17. The analysis confirms the importance of CH_3NH_2 (+M) $\rightleftarrows CH_3 + NH_2$ (+M) R1b, CH_2NH_2 + M $\rightleftarrows$ CH_2 NH + H + M (R10), and $CH_2NH_2 + CH_2NH_2 \rightarrow$ adduct (R13). While recombination of CH_2NH_2 to form an adduct (R13) is conceivably important under these conditions, it is insignificant at higher temperatures and dilute conditions, such as in the flow reactor experiments of Marrodán et al. (Figure 15).

4 | CONCLUDING REMARKS

Co-combustion of ammonia with natural gas may be an attractive option in spark-ignited engines and other applications. By analogy with other ammonia/co-fuel systems, H-abstraction from the fuel ($CH_4 + NH_2 \rightleftarrows CH_3 + NH_3$) may have an impact on the ignition process. However, the subsequent radical–radical reactions $CH_x + NH_y$ will be important for the fate of the reactive nitrogen, that is, whether it is converted through amine oxidation or feeds into the hydrocarbon amine/cyanide pool. The key step is the reaction between CH_3 and NH_2, which has multiple product channels; the major ones being CH_3NH_2 (+M) (R1), CH_2NH_2 + H (R11b), and CH_4 + NH (R31). In this work, it has been possible to constrain the rate constants for several of these steps, facilitating a more reliable assessment of the fate of the N-atom in this reaction. Figure 19 shows an Arrhenius plot for $CH_3 + NH_2$. According to our present understanding, recombination of CH_3 and NH_2 to form methylamine (R1) dominates up to about 1400 K at atmospheric pressure and below 2000 K at 100 atm. At sufficiently high temperature, H-abstraction to form CH_4 + NH (R31) and addition–elimination to form CH_2NH_2 + H (R11b), with similar rate constants, become competitive.

The implication of these results is that methylamine can be expected to be an important intermediate in co-combustion of natural gas and ammonia, and more work on the chemistry of CH_3NH_2 is desirable.

ACKNOWLEDGMENTS

The authors acknowledge support from the European Horizon 2020 program for the Engimmonia project. M.U.A. expresses her gratitude to Grant PID2021-124320BI00, funded by MCIN/AEI/10.13039/501100011033 and "ERDF A way of making Europe," by the European Union and to Aragon Government.

DATA AVAILABILITY STATEMENT

Data sharing not applicable to this article as no datasets were generated or analyzed during the current study.

ORCID

Peter Glarborg https://orcid.org/0000-0002-6856-852X

REFERENCES

1. Valera-Medina A, Xiao H, Owen-Jones M, David WIF, Bowen PJ. Ammonia for power. *Prog Energy Combust Sci*. 2018;69:63-102.
2. Kobayashi H, Hayakawa A, Somarathne KKA, Okafor EC. Science and technology of ammonia combustion. *Proc Combust Inst*. 2019;37:109-133.
3. Valera-Medina A, Amer-Hatem F, Azad AK, et al. A review on ammonia as a potential fuel: from synthesis to economics. *Energy Fuels*. 2021;35:6964-7029.
4. Chai WS, Bao Y, Jin P, Tang G, Zhou L. A review on ammonia, ammonia-hydrogen and ammonia-methane fuels. *Renew Sustain Energy Rev*. 2021;147:111254.
5. Kang L, Pan W, Zhang J, Wang W, Tang C. A review on ammonia blends combustion for industrial applications. *Fuel*. 2023;332:126150.
6. Dai L, Gersen S, Glarborg P, Mokhov A, Levinsky H. Autoignition studies of NH_3/CH_4 mixtures at high pressure. *Combust Flame*. 2020;218:19-26.
7. Shu B, He X, Ramos CF, Fernandes RX, Costa M. Experimental and modeling study on the auto-ignition properties of ammonia/methane mixtures at elevated pressures. *Proc Combust Inst*. 2021;38:261-268.
8. Liao W, Wang Y, Chu Z, Yang B. Investigating auto-ignition characteristics and kinetic modeling of NH_3/CH_4 mixtures using an RCM. *Combust Flame*. 2024;260:113257.
9. Liu B, Zhou M, Zhang Z, Mi X, Belal BY, Li G. Ignition delay times and chemical reaction kinetic analysis for the ammonia–natural gas blends. *Energy Fuels*. 2024;38:1373-1382.
10. Xiao H, Lai S, Valera-Medina A, Li J, Liu J, Fu H. Experimental and modeling study on ignition delay of ammonia/methane fuels. *Int J Energy Res*. 2020;44:6939-6949.
11. Liu J, Zou C, Luo J. Experimental and modeling study on the ignition delay times of ammonia/methane mixtures at high dilution and high temperatures. *Proc Combust Inst*. 2023;39:4399-4407.
12. Jiang Z, Dong S, Gao W, et al. Probing the effect of fuel components on the auto-ignition behavior of ammonia/natural gas blends: a case study of ethane addition. *Combust Flame*. 2024;259:113186.
13. Mendiara T, Glarborg P. Ammonia chemistry in oxy-fuel combustion of methane. *Combust Flame*. 2009;156:1937-1949.
14. Sun Z, Xu J, Su S, et al. Formation and reduction of NO from the oxidation of NH_3/CH_4 with high concentration of H_2O. *Fuel*. 2019;247:19-25.
15. Arunthanayothin S, Stagni A, Song Y, Herbinet O, Faravelli T, Battin-Leclerc F. Ammonia–methane interaction in jet-stirred and flow reactors: an experimental and kinetic modeling study. *Proc Combust Inst*. 2021;38:345-353.
16. García-Ruiz P, Salas I, Casanova E, Bilbao R, Alzueta M. Experimental and modeling high-pressure study of ammonia–methane oxidation in a flow reactor. *Energy Fuels*. 2024;38:1399-1415.
17. Jin S, Tu Y, Liu H. Experimental study and kinetic modeling of NH_3/CH_4 co-oxidation in a jet-stirred reactor. *Int J Hydrogen Energy*. 2022;47:36323-36341.
18. Zhou S, Yang W, Zheng S, et al. An experimental and kinetic modeling study on the low and intermediate temperatures oxidation of $NH_3/O_2/Ar$, $NH_3/H_2/O_2/Ar$, $NH_3/CO/O_2/Ar$, and $NH_3/CH_4/O_2/Ar$ mixtures in a jet-stirred reactor. *Combust Flame*. 2023;248:112529.
19. Jin S, Tu Y, Liu H. Experimental and numerical study of the effect of H_2O and CO_2 dilution on NH_3/CH_4 co-oxidation characteristics in a jet-stirred reactor. *Int J Hydrogen Energy*. 2024;49:621-635.
20. Okafor EC, Naito Y, Colson S, et al. Experimental and numerical study of the laminar burning velocity of CH_4-NH_3–air premixed flames. *Combust Flame*. 2018;187:185-198.
21. Okafor EC, Naito Y, Colson S, et al. Measurement and modelling of the laminar burning velocity of methane-ammonia-air flames at high pressures using a reduced reaction mechanism. *Combust Flame*. 2019;204:162-175.
22. Han X, Wang Z, Costa M, Sun Z, He Y, Cen K. Experimental and kinetic modeling study of laminar burning velocities of NH_3/air, NH_3/H_2/air, NH_3/CO/air and NH_3/CH_4/air premixed flames. *Combust Flame*. 2019;206:214-226.
23. Lubrano Lavadera M, Han X, Konnov AA. Comparative effect of ammonia addition on the laminar burning velocities of methane, n-heptane, and iso-octane. *Energy Fuels*. 2020;35:7156-7168.
24. Zhang X, Wang J, Chen Y, Li C. Effect of CH_4, pressure, and initial temperature on the laminar flame speed of an NH_3–air mixture. *ACS Omega*. 2021;6:11857-11868.
25. Shu T, Xue Y, Zhou Z, Ren Z. An experimental study of laminar ammonia/methane/air premixed flames using expanding spherical flames. *Fuel*. 2021;290:120003.
26. Rocha RC, Zhong S, Xu L, et al. Structure and laminar flame speed of an ammonia/methane/air premixed flame under varying pressure and equivalence ratio. *Energy Fuels*. 2021;35:7179-7192.
27. Wang D, Wang Z, Zhang T, et al. A comparative study on the laminar C_1–C_4 n-alkane/NH_3 premixed flame. *Fuel*. 2022;324:124732.
28. Wang S, Wang Z, Chen C, Elbaz AM, Sun Z, Roberts WL. Applying heat flux method to laminar burning velocity measurements of NH_3/CH_4/air at elevated pressures and kinetic modeling study. *Combust Flame*. 2022;236:111788.
29. Han X, Feng H, Lin R, Konnov AA. A new correlation between diluent fraction and laminar burning velocities: example of CH_4, NH_3, and $CH_4 + NH_3$ flames diluted by N_2. *Fuel*. 2024;364:131108.

30. Zhou Q, Tian J, Zhang X, et al. Investigation of the ammonia-methane-air laminar burning characteristics at high temperatures and pressures. *Fuel*. 2024;365:130987.
31. Figueroa-Labastida M, Zheng L, Streicher JW, Hanson RK. High-temperature laminar flame speed measurements of ammonia/methane blends behind reflected shock waves. *Combust Flame*. 2024;261:113314.
32. Tian Z, Li Y, Zhang L, Glarborg P, Qi F. An experimental and kinetic modeling study of premixed $NH_3/CH_4/O_2/Ar$ flames at low pressure. *Combust Flame*. 2009;156:1413-1426.
33. Lamoureux N, Marschallek-Watroba K, Desgroux P, Pauwels J-F, Sylla MD, Gasnot L. Measurements and modelling of nitrogen species in $CH_4/O_2/N_2$ flames doped with NO, NH_3, or NH_3 + NO. *Combust Flame*. 2017;176:48-59.
34. Rao G, Dong M, Nie W, Lin X, Liang Y, Lu J. Study on the mechanism of nitrogen conversion in NH_3-doped methane premixed flame based on multi-spectral analysis methods. *J Energy Inst*. 2023;111:101437.
35. Wang S, Wang Z, Roberts WL. Measurements and simulations on effects of elevated pressure and strain rate on NO_x emissions in laminar premixed NH_3/CH_4/air and NH_3/H_2/air flames. *Fuel*. 2024;357:130036.
36. Zhang X, Yalamanchi KK, Sarathy SM. Combustion chemistry of ammonia/C_1 fuels: a comprehensive kinetic modeling study. *Fuel*. 2023;341:127676.
37. Emeleus HJ, Jolley LJ. Kinetics of the thermal decomposition of methylamine. *J Chem Soc*. 1935;929-935.
38. Marrodán L, Pérez T, Alzueta MU. Conversion of methylamine in a flow reactor and its interaction with NO. *Combust Flame*. 2024;259:113130.
39. Dorko EA, Pchelkin NR, Wert JC, Mueller GW. Initial shock tube studies of monomethylamine. *J Phys Chem*. 1979;83:297-302.
40. Higashihara T, Gardiner WC, Hwang SM. Shock tube and modeling study of methylamine thermal decomposition. *J Phys Chem*. 1987;91:1900-1905.
41. Klatt M, Spindler B, Wagner HG. Minor decomposition channels of CH_3NH_2 at high temperatures. *Z Phys Chem*. 1995;191:241-249.
42. Votsmeier M, Song S, Davidson DF, Hanson RK. Shock tube study of monomethylamine thermal decomposition and NH_2 high temperature absorption coefficient. *Int J Chem Kin*. 1999;31:323-330.
43. Glarborg P, Miller JA, Ruscic B, Klippenstein SJ. Modeling nitrogen chemistry in combustion. *Prog Energy Combust Sci*. 2018;67:31-68.
44. Lucassen A, Zhang K, Warkentin J, et al. Fuel-nitrogen conversion in the combustion of small amines using dimethylamine and ethylamine as biomass-related model fuels. *Combust Flame*. 2012;159:2254-2279.
45. Glarborg P, Andreasen CS, Hashemi H, Qian R, Marshall P. Oxidation of methylamine. *Int J Chem Kin*. 2020;52:893-906.
46. Jian J, Hashemi H, Wu H, Glarborg P, Jasper AW, Klippenstein SJ. An experimental, theoretical, kinetic modeling study of post-flame oxidation of ammonia. *Combust Flame*. 2024;261:113325.
47. Dean AM, Bozzelli JW. Combustion chemistry of nitrogen. In: Gardiner WC, ed. *Gas Phase Combustion Chemistry*. Springer-Verlag; 2000.
48. Sun H, Vaghjiani GL, Law CK. Ab initio kinetics of methylamine radical thermal decomposition and H-abstraction from monomethylhydrazine by H-atom. *J Phys Chem A*. 2020;124:3747-3753.
49. Dievart P, Catoire L. Contributions of experimental data obtained in concentrated mixtures to kinetic studies: application to monomethylhydrazine pyrolysis. *J Phys Chem A*. 2020;124:6214-6236.
50. Li S, Davidson DF, Hanson RK. Shock tube study of ethylamine pyrolysis and oxidation. *Combust Flame*. 2014;161:2512-2518.
51. Zhang ZP, Wang SH, Shang YL, Liu JH, Luo SN. Theoretical study on ethylamine dissociation reactions using VRC-VTST and SS-QRRK methods. *J Phys Chem A*. 2024;128:2191-2199.
52. Pappijn CAR, Vermeire FH, Van de Vijver R, Reyniers M-F, Marin GB, Van Geem KM. Combustion of ethylamine, dimethylamine and diethylamine: theoretical and kinetic modeling study. *Proc Combust Inst*. 2021;38:585-592.
53. Rawadieh SE, Altarawneh M, Altarawneh IS, Shiroudi A, El-Nahas AM. Exploring reactions of amines-model compounds with NH_2: in relevance to nitrogen conversion chemistry in biomass. *Fuel*. 2021;291:120076.
54. Bosco SR, Nava DF, Brobst WD, Stief LJ. Temperature and pressure dependence of the absolute rate constant for the reactions of NH_2 radicals with acetylene and ethylene. *J Chem Phys*. 1984;81:3505-3511.
55. Song S, Golden DM, Hanson RK, et al. A shock tube study of the reaction $NH_2 + CH_4 \rightarrow NH_3 + CH_3$ and comparison with transition state theory. *Int J Chem Kinet*. 2003;35:304-309.
56. Xu Z-F, Li S-M, Yu Y-X, Li Z-S, Sun C-C. Theoretical studies on the reaction path dynamics and variational transition-state theory rate constants of the hydrogen-abstraction reactions of the NH(X3Σ-) radical with methane and ethane. *J Phys Chem A*. 1999;103:4910-4917.
57. Klippenstein SJ, Georgievskii Y, Harding LB. Predictive theory for the combination kinetics of two alkyl radicals. *Phys Chem Chem Phys*. 2006;8:1133-1147.
58. Jodkowski JT, Ratajczak E, Fagerström K, et al. Kinetics of the cross reaction between amidogen and methyl radicals. *Chem Phys Lett*. 1995;240:63-71.
59. de Jesus DN, da Silva JMBA, Tejero TN, Machado GdS, Xavier NF Jr., Bauerfeldt GF. Chemical mechanism for the decomposition of CH_3NH_2 and implications to interstellar glycine. *Mon Not Royal Astron Soc*. 2021;501:1202-1214.
60. Blumenberg B, Wagner HG. Reaction of methylamine with hydrogen atoms. *Ber Bunsenges Phys Chem*. 1973;77:253-257.
61. Zhang Q, Zhang RQ, Chan KS, Bello I. Ab initio and variational transition state approach to β-C_3N_4 formation: kinetics for the reaction of CH_3NH_2 with H. *J Phys Chem A*. 2005;109:9112-9117.
62. Kerkeni B, Clary DC. Quantum scattering study of the abstraction reactions of H atoms from CH_3NH_2. *Chem Phys Lett*. 2007;438:1-7.
63. Zhao M, Ning H, Shang Y, Shi J. Accurate reaction barriers and rate constants of H-abstraction from primary, secondary, and tertiary amines by H atom determined with the isodesmic reaction method. *Chem Phys Lett*. 2021;776:138708.
64. Gray P, Thynne JCJ. Hydrogen and deuterium atom abstraction from methylamine and deuterated methylamines. Kinetic isotope effects and relative reactivities of the methyl and amine groups. *Trans Faraday Soc*. 1963;59:2275-2286.

65. Gray P, Thynne JCJ. Arrhenius parameters for elementary combustion reactions: H-atom abstraction from NH bonds. *Symp (Int) Combust*. 1965;10:435-443.
66. Röhrig M, Wagner HG. A kinetic study about the reactions of NH with hydrocarbons part 1: saturated hydrocarbons and acetaldehyde. *Ber Bunsenges Phys Chem*. 1994;98:858-863.
67. Almatarneh MH, Altarawneh M, Poirier RA, Saraireh IA. High level ab initio, DFT, and RRKM calculations for the unimolecular decomposition reaction of ethylamine. *J Comput Sci*. 2014;5:568-575.
68. Altarawneh M, Almatarneh MH, Marashdeh A, Dlugogorski BZ. Decomposition of ethylamine through bimolecular reactions. *Combust Flame*. 2016;163:532-539.
69. Glarborg P, Hashemi H, Marshall P. Challenges in kinetic modeling of ammonia pyrolysis. *Fuel Commun*. 2022;10:100049.
70. Kim KP, Michael JV. The thermal reactions of CH_3. *Symp (Int) Combust*. 1994;25:713-719.
71. Davidson DF, Di Rosa MD, Chang EJ, Hanson RK, Bowman CT. A shock tube study of methyl-methyl reactions between 1200 and 2400 K. *Int J Chem Kinet*. 1995;27:1179-1196.
72. Marshall P, Rawling G, Glarborg P. New reactions of diazene and related species for modelling combustion of amine fuels. *Mol Phys*. 2021;119:e1979674.
73. Karton A, Daon S, Martin JML. W4-11: A high-confidence benchmark dataset for computational thermochemistry derived from first-principles W4 data. *Chem Phys Lett*. 2011;510:165-178.
74. Klippenstein SJ, Harding LB, Ruscic B. Ab initio computations and active thermochemical tables hand in hand: heats of formation of core combustion species. *J Phys Chem A*. 2017;121:6580-6602.
75. Glarborg P, Hashemi H, Cheskis S, Jasper AW. On the rate constant for NH_2 + HO_2 and third-body collision efficiencies for NH_2 + H (+M) and NH_2 + NH_2 (+M). *J Phys Chem A*. 2021;125:1505-1516.
76. Jasper AW. Predicting third-body collision efficiencies for water and other polyatomic baths. *Faraday Discuss*. 2022;238:68-86.

How to cite this article: Glarborg P, Alzueta MU. Decomposition of CH_3NH_2: Implications for CH_x/NH_y radical–radical reactions. *Int J Chem Kinet*. 2024;1-14. https://doi.org/10.1002/kin.21760